When does nanofluidic memory disappear? Understanding and reinstating memristive behavior of ionic liquids in two-dimensional nanochannels

Abdulghani Ismail[1,2,3¥], Jing Yang[4,5¥], Kalluvadi Veetil Saurav[2,4], Louis Maduro[1,2], Hiran Jyothilal[1,2], Robert A. W. Dryfe[4,5], Ashok Keerthi[2,4,6], Boya Radha[1,2,6*]

[1] Department of Physics and Astronomy, School of Natural Sciences, The University of Manchester, Manchester M13 9PL, United Kingdom
[2] National Graphene Institute, The University of Manchester, Manchester M13 9PL, United Kingdom

[3] Univ. Paris-Saclay, CNRS, Institut Galien Paris-Saclay, Orsay 91400, France

[4] Department of Chemistry, School of Natural Sciences, The University of Manchester, Manchester M13 9PL, United Kingdom

[5] Henry Royce Institute, University of Manchester, Manchester, M13 9PL, United Kingdom
[6] Photon Science Institute, The University of Manchester, Manchester M13 9PL, United Kingdom

[¥] These authors equally contributed

*Correspondence to be addressed to: radha.boya@manchester.ac.uk

Experimental

Fabrication of 2D nanocapillary devices

The devices were produced as described elsewhere [1]. Briefly, we exfoliate the 2D materials, bottom, spacer, and top, by mechanical exfoliation . First, a suspended SiN_x/Si membrane (thickness 500 nm) was patterned by photolithography and reactive ion etching (RIE) to open an elongated aperture of ~3 × 25 μm that serves as the entry/exit to channels. A hBN or graphite flake was then transferred onto the SiN_x membrane and etched from the backside to reopen the access on the hole side and define the inlet region of the future nanochannels. Next, a graphene flake on Si/SiO_2 substrate was patterned into parallel stripes ~110 nm wide and separated by ~170 nm using electron-beam lithography followed by dry etching; these ribbons act as spacers defining the channel width. A second hBN flake (thickness ~120 nm) was subsequently transferred onto the patterned graphene, forming a top-spacer stack that was aligned and placed perpendicularly to the membrane aperture onto the bottom 2D crystal, thereby generating an array of parallel slit nanochannels. To define the channel length, a Cr/Au (5/60 nm) film was deposited by photolithography and metal evaporation, after which exposed region of the 2D layers were removed by dry etching. Channel lengths were in the order of ~5μm. The electrolyte entrance was then cleared by etching the graphene spacer above the hole from the backside using oxygen plasma. Finally, the completed stack was annealed in a reducing atmosphere (10% H_2) at 300 °C for 3 h and then at 400 °C for 3 h to

remove polymer residues and improve adhesion between layers. The resulting structure is a multilayer 2D nanocapillary device suitable for ionic transport measurements.

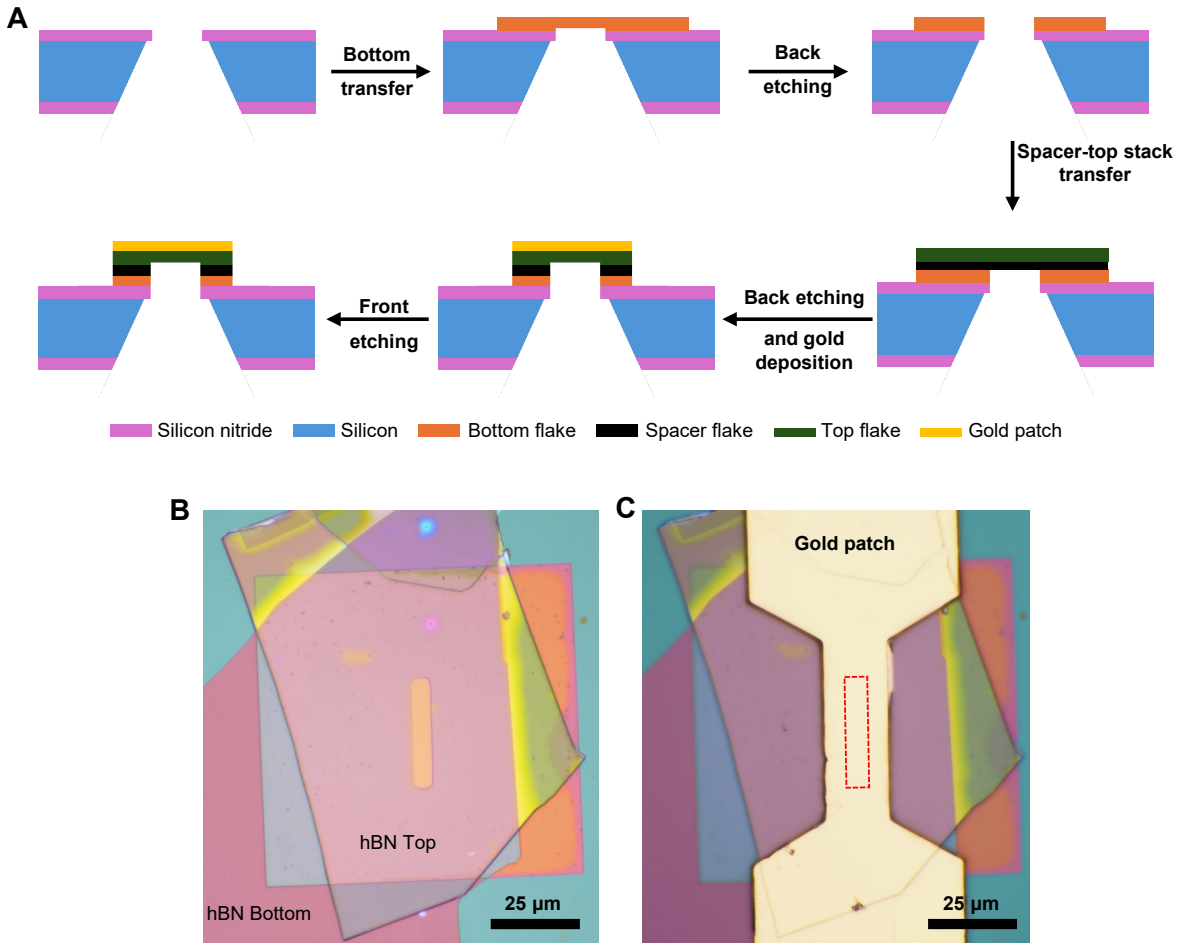

Figure. S1 Fabrication of a two-dimensional nanochannel device. **(A)** shows the steps involved in the fabrication of a two-dimensional nanochannel device, wherein initially a bottom flake is transferred onto a free-standing SiNx membrane with a micro-hole. The bottom flake is then back-etched to allow a path for fluid to enter the nanochannel. Further, a stack of top flake and spacer is transferred onto the bottom flake and dry etched from the back side to remove the spacer present on the micro-hole aperture. To define channel length and mask the stack during further etch, Cr (5 nm)/Au (50 nm) is deposited onto this tri-layer stack, followed by front etching to remove the exposed region. **(B)** and **(C)** shows an optical image of a trilayer stack of hBN top, graphene spacer and hBN bottom before and after Cr/Au deposition. The red coloured dashed lines in image (**C)** show the micro-hole aperture.

Materials and chemicals

Lithium bis(trifluoromethanesulfonyl)imide (LiTFSI, 99%) was obtained from Fluorochem. 1-Ethyl-3-methylimidazolium chloride ([EMIM]Cl, ≥95%), acetonitrile (ACN, 99.9%), potassium chloride (KCl), sulfuric acid (H_2SO_4), dimethyl carbonate (DMC, 99%), diethyl carbonate (DEC, 99%) and acetone (≥99.8%) were purchased from Sigma-Aldrich. Dimethyl sulfoxide (DMSO, ≥99.5%) with water content ≤0.2% was purchased from Thermo Fisher Scientific. Ultrapure water with a resistivity of 18.2 MΩ·cm was produced using a Milli-Q purification system.

Structural characterization

Surface topography and thickness of the spacer were further characterized by tapping-mode atomic force microscopy (AFM) on a Dimension FastScan instrument (Bruker, USA).

Results

Variation of frequency

The variation of the I-V characteristics with variation of frequency is shown in Figures S1-3 below under different conditions presenting pinched hysterises. All the conditions showed variation of the hysteresis with changing frequency. Additionally, capacitive loop always occurred at high frequencies thus masking part of the memristive loop.

In a delaminated device (experimental conductance at low voltage higher than theoretical conductance and no selectivity between cations and anions) saturation loop style was seen with RTIL and KCl on both sides of the nanochannels (asymmetric condition) contrary to mixed Crossing / Wien observed in confined nanochannels. This result is similar to the earlier reports of observation of saturation style under low/no confinement in thick nanochannels and microchannels shown in literature [2-4].

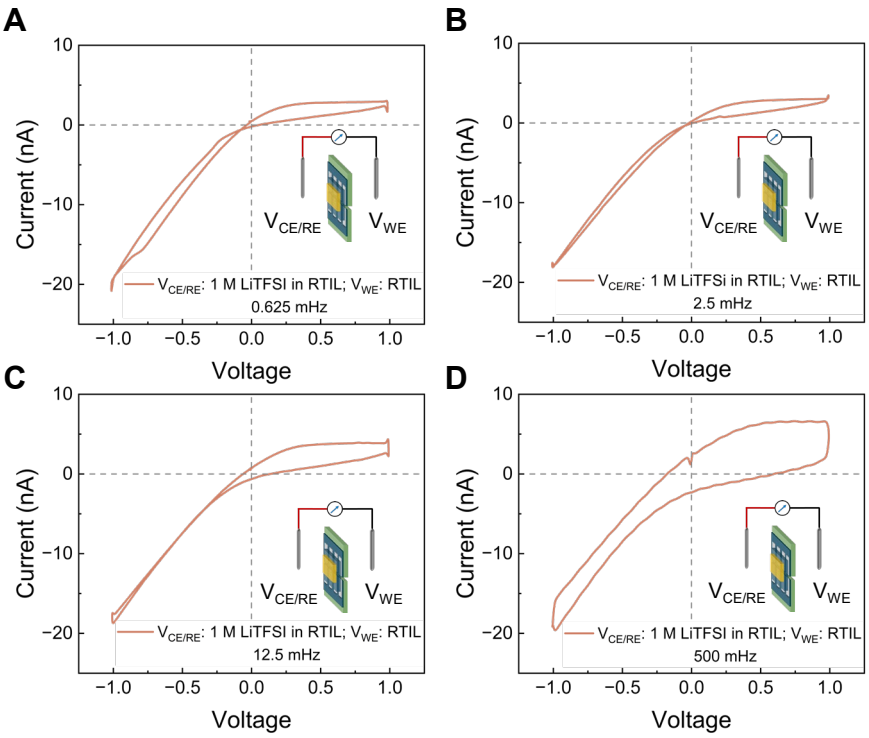

Figure S2: Effect of variation of frequency on pinched loop in asymmetric electrolyte in RTIL conditions. Variation of frequency between 0.625 and 500 mHz under alternative triangular voltage conditions in hBN/Gr/hBN (top/spacer/bottom) device with h= 0.7 nm. Asymmetric conditions were achieved by adding different concentrations of LiTFSI on either side of the device: 0M LiTFSI in RTIL (hole side) / 1 M LiTFSI in RTIL (device side. Under these asymmetric conditions, the observed memristive behavior corresponded to a crossing-1 type loop, whereas only capacitive I-V curves without pinching were observed high frequency (500 mHz).

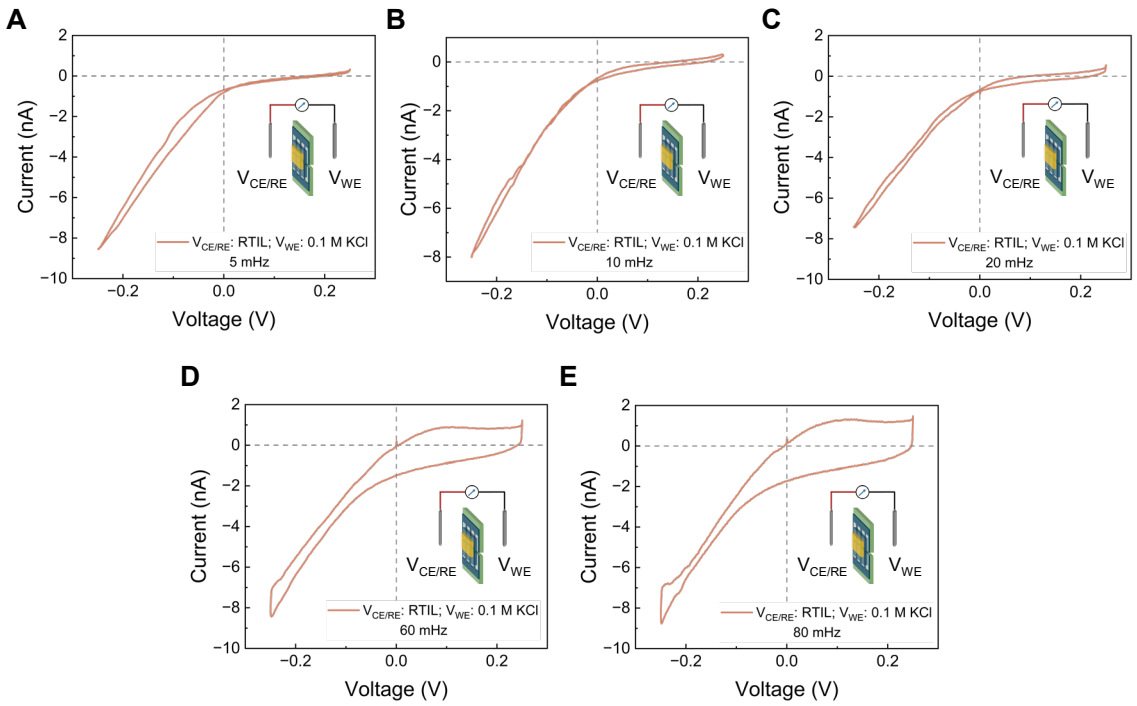

Figure S3: Effect of the variation of frequency on pinched loop in asymmetric RTIL/aqueous electrolyte conditions. Variation of frequency between 5 and 80 mHz under alternative triangular voltage conditions in hBN/Gr/Gr (top/spacer/bottom) device with h = 1.4 nm. Here, asymmetry is achieved by adding RTIL (EMIM-TFSI) (device side) / 0.1M KCl (aq) (hole side).

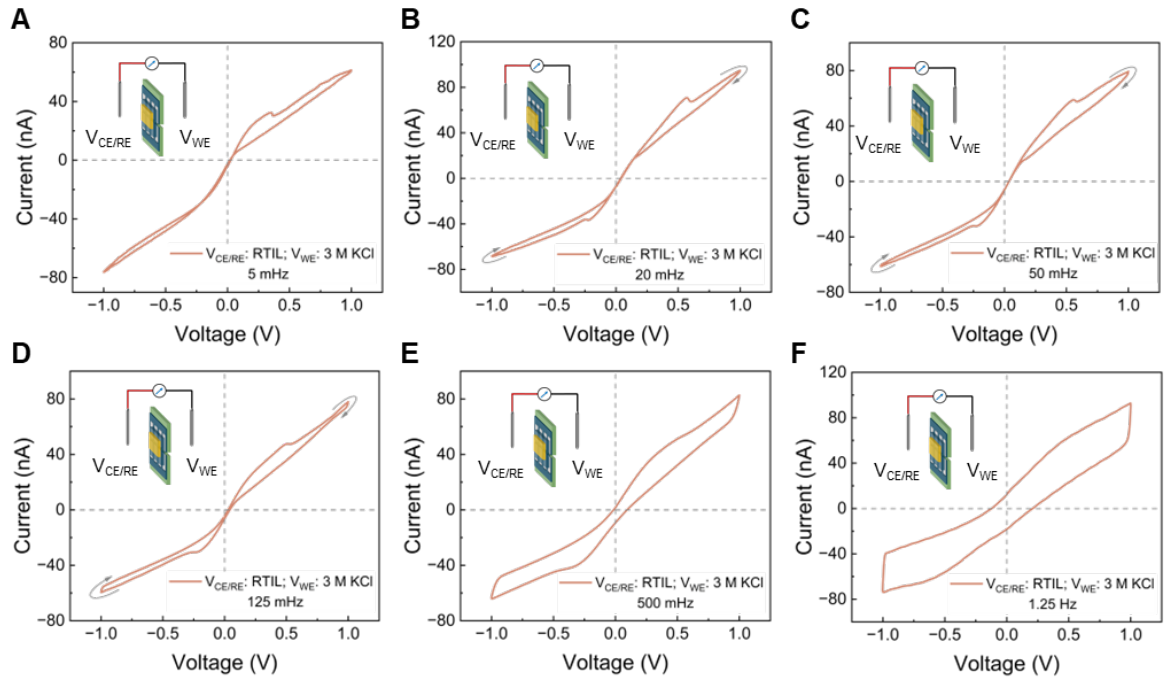

Figure S4: Effect of variation of frequency on pinched loop in asymmetric RTIL/aqueous electrolyte conditions in delaminated device. Variation of frequency between 5 mHz and 1.25 Hz under alternative triangular voltage conditions in hBN/Gr/hBN (top/spacer/bottom) device with h = 1.7 nm. The device is showing higher conductance and no selectivity signifying its delamination so the actual nanochannel height is different than its state of fabrication. Asymmetric conditions were made by adding RTIL (EMIM-TFSI) (device side) / 3M KCl (aq) (hole side).

Variation of measurement electrode Type

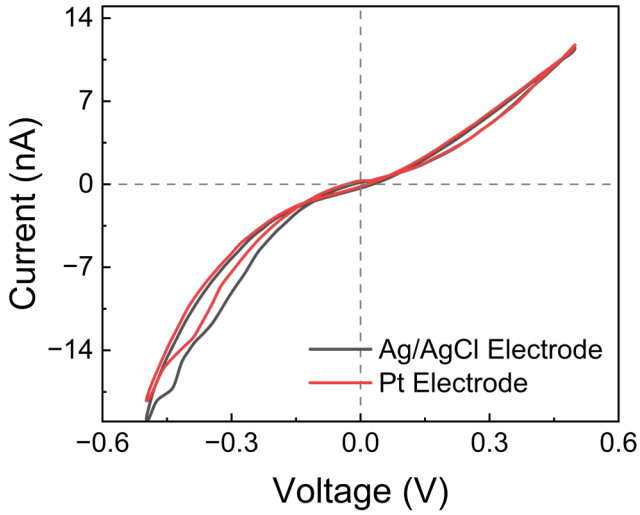

Figure S5: Effect of variation of electrode type on the IV characteristics. Two electrode types were tested: Ag/AgCl and Pt. Alternative triangular voltage was employed using 1M KCl (aq) as electrolyte and hBN/Gr/Gr (top/spacer/bottom) device with h = 1.4 nm.

Dilution of EMIM-TFSI (RTIL) in different solvents

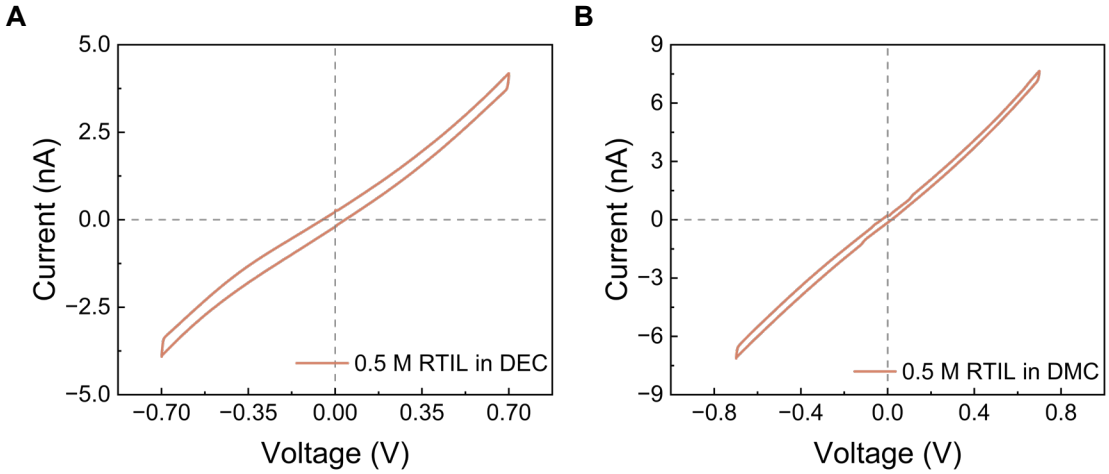

Figure S6: Effect of variation of solvent when dilution RTIL on the pinched hysterisis. EMIM-TFSI RTIL was diluted to concentration 0.5 M using diethyl carbonate (DEC) and dimethyl carbonate (DMC) solvents where the IV characteristic showed non-pinched loop reflecting capacitive behaviour. hBN/Gr/Gr (top/spacer/bottom) device with h = 1.4 nm was used.

Repeatability and time-drift in mixed conditions

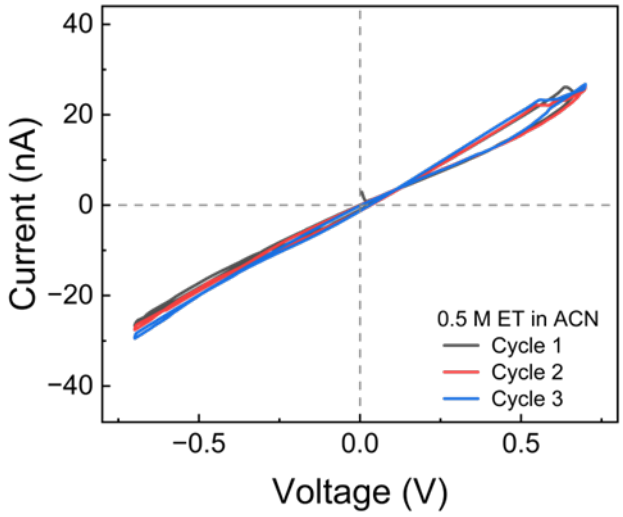

Figure S7: Repeatability of three consecutive IV cycles. Three consecutive IV cycles of 0.5 M of EMIM-TFSI dissolved in acetonitrile. cyclic voltammetry using a triangular voltage waveform with a scan rate of 20 mV/s (equivalent to a frequency of 7.1 mHz). Measurements were performed in hBN/graphene/graphene (top/spacer/bottom) device with a channel height h= 1.4 nm, corresponding to the graphene spacer thickness.

References

1. Bhardwaj, A., et al., *Fabrication of angstrom-scale two-dimensional channels for mass transport.* Nature protocols, 2024. **19**(1): p. 240-280.
2. Li, P., et al., *Artificial funnel nanochannel device emulates synaptic behavior.* Nano Letters, 2024. **24**(20): p. 6192-6200.
3. Sheng, Q., et al., *Transporting an ionic-liquid/water mixture in a conical nanochannel: a nanofluidic memristor.* Chemical Communications, 2017. **53**(45): p. 6125-6127.
4. Liu, W., et al., *A droplet memristor with ionic liquid-electrolyte meniscus.* Chemical Engineering Journal, 2025. **504**: p. 158948.